Comparative analysis of two-phase expansion and sub-critical organic Rankine cycle systems for solar and geothermal applications

Desai, Nishith B.; Tammone, Carlotta; Haglind, Fredrik

Published in:
Proceedings of ECOS 2022 - The 35th International Conference on Efficiency, Cost, Optimization, Simulation and Environmental Impact of Energy Systems 2022

Publication date:
2022

Document Version
Peer reviewed version

Comparative analysis of two-phase expansion and sub-critical organic Rankine cycle systems for solar and geothermal applications

Nishith B. Desai[a], Carlotta Tammone[b] and Fredrik Haglind[c]

[a]Technical University of Denmark, Department of Civil and Mechanical Engineering , 2800 Kongens Lyngby, Denmark, nbdes@mek.dtu.dk, CA
[b]Technical University of Denmark, Department of Civil and Mechanical Engineering, 2800 Kongens Lyngby, Denmark, carta@mek.dtu.dk
[c]Technical University of Denmark, Department of Civil and Mechanical Engineering, 2800 Kongens Lyngby, Denmark, frh@mek.dtu.dk

Abstract:

For low to medium temperature heat sources (up to about 300 °C), the organic Rankine cycle technology is a cost-effective option for power generation. In addition to conventional sub-critical organic Rankine cycle systems, cycle architectures characterized by two-phase expansion, like, trilateral and partial evaporation organic Rankine cycles, have been proposed. These cycle architectures results in a higher utilization of the available heat and subsequently in a higher exergy efficiency of the system compared to that of sub-critical organic Rankine cycle systems. However, these configurations have a higher cost of the power system, and lower isentropic efficiency of the expander compared to the sub-critical organic Rankine cycle based configurations. This paper presents a techno-economic comparison among trilateral, partial evaporation and sub-critical organic Rankine cycle systems considering concentrated solar power and geothermal heat sources, respectively. A selection method for these configurations is proposed, helping to select the optimal power cycle for concentrated solar power and geothermal plants. The results suggest that the subcritical organic Rankine cycle system is the preferred choice over the trilateral and partial evaporation organic Rankine cycles for concentrated solar power plants. As for the geothermal energy powered plants, the results indicate that for 10 % penalty in expander isentropic efficiency, the specific cost of the trilateral organic Rankine cycle system should be equal or lower than that of the subcritical organic Rankine cycle system in order to become favourable. In addition, high values of the condensation temperature are favourable for the trilateral and partial evaporation organic Rankine cycles.

Keywords:

Concentrated solar power; Geothermal energy; Organic Rankine cycle; Renewable energy.

1. Introduction

Concentrated solar power (CSP) with thermal energy storage (TES) and geothermal energy are renewable energy sources that can provide a high capacity factor. From a techno-economic perspective, a recently proposed micro-structured polymer foil-based CSP systems [1] may offer advantages for medium temperature and medium-scale dispatchable (on demand) applications compared to the conventional mirror based CSP systems [2]. Due to the high upfront costs of geothermal and medium temperature and medium-scale CSP plants, the adoption of better performing power systems is crucial to recover the high capital investment costs. In this regard, power cycles with no evaporation or partial evaporation of the working fluid at the inlet of the expander for low to medium temperature heat sources have been proposed in literature. The trilateral cycle, where the expansion starts from saturated liquid conditions, achieves theoretically the highest exergy efficiency when extracting power from low temperature heat sources with finite heat capacity [3]. By removing/minimizing the constant temperature vaporization of the power cycle working fluid, a better match between the heat source and power cycle working fluid temperature profiles (hot and cold streams) can be achieved during the heat exchange. As a result, the irreversibilities decrease and the amount of exchanged heat increases. However, the disadvantages of the trilateral cycle are that it requires more voluminous and costly power systems due to the increase in heat exchange area and number of stages of the expander compared to the conventional subcritical power cycles. In addition, the two-phase expansion leads to the degradation of the performance of the expander and the technology is still at an early development stage. In order to partially overcome some of the challenges posed by trilateral cycle systems, the partial evaporation cycle has been proposed as a modification of the conventional subcritical cycle,

where the power cycle working fluid is partially evaporated and expanded in the two-phase region. The partial evaporation cycle based systems have shown promising techno-economic performance compared to the trilateral cycle based systems due to the requirement of a lower mass flow rate of working fluid for the same heat transfer rate with the heat source, lower heat exchanger areas and higher efficiency and lower cost of the expander [4].

Fischer [5] investigated trilateral cycles for heat source temperatures in the range from 150 °C to 350 °C and concluded that organic fluids perform better compared to water as working fluids for trilateral cycles. They also reported that for the trilateral organic Rankine cycle (TLORC) the exergy efficiency for power generation is 14 % to 29 % higher than that of the conventional subcritical organic Rankine cycle (SCORC). Lai and Fischer [6] proved that siloxanes achieve higher exergy efficiencies for TLORC with respect to water; however, the power system runs with siloxanes and is therefore expected to be more costly due to very high volume ratio across the expander and condensation pressures well below atmospheric pressure. On the other hand, alkanes and light hydrocarbons achieved slightly lower efficiencies but also lower volumetric flow rate change across the expander and higher condensation pressures than that of siloxanes. In the first attempt to evaluate the economic feasibility of trilateral cycle systems, Lecompte et al. [7] found that the specific investment cost for the TLORC system is 19 % higher than that of the SCORC system for a low temperature heat source, namely water at 100 °C. In a comprehensive study on a wide range of heat source temperatures, Lecompte et al. [8] reported that for heat source temperatures below 250 °C, the TLORC outperforms the partial evaporation organic Rankine cycle (PEORC) based on the thermodynamic performance, considering a fixed isentropic efficiency of the expander. Yari et al. [9] studied the impact of the expander efficiency on the system performance and cost. Their results suggested that a decrease in expander efficiency from 85 % to 65 % results in a decrease in net power output by 40 % and in an increase in specific investment cost by 25 %. For geothermal energy powered PEORC systems, Tammone et al. [4] reported that PEORC systems are able to provide an increase in the net power output between 20 % to 60 % compared with SCORC systems for the considered heat source temperatures, but also that PEORC systems are associated with higher specific investment costs (up to 50 %) than SCORC systems. They also highlighted that when the performance of the expander is not significantly affected by the two-phase expansion, the PEORC system achieves up to 15 % lower levelized cost of electricity (LCOE) compared to the SCORC system depending on the geothermal heat source extraction and re-injection temperatures.

As for CSP plants with a TLORC/PEORC system, the better match between heat source profile and ORC working fluid profile leads to a lower average temperature of the heat addition in the solar field and a higher temperature difference between the top and bottom temperature for the thermal energy storage system than that of CSP plants with a SCORC system. As a result, a higher solar field efficiency and a lower cost of the TES system for the same storage capacity requirement can be achieved for TLORC/PEORC systems than those of the SCORC based CSP plants. However, as the TLORC and PEORC architectures also result in a more voluminous and costly organic Rankine cycle system and a degradation of the performance of the expander, there is a need to carry out techno-economic analyses in order to properly evaluate the feasibility of TLORC/PEORC systems for CSP applications. As far as geothermal plants are concerned, there is a need to study the effects of the expander efficiency and the cost of the power system on the selection of ORC architectures considering relevant parameters of the geothermal plants.

In this paper we present a techno-economic comparison among TEORC, PEORC and SCORC systems considering a CSP plant with packed-bed rock TES and geothermal energy heat sources, respectively. A novel approach based on the development of a selection diagram is proposed, capturing the influence of the relative specific power systems cost and the relative isentropic efficiency of the expanders on the LCOE. The novel contributions of our work to state of the art are as follows:

- A techno-economic comparison among subcritical, trilateral and partial evaporation ORC architectures powered by foil-based CSP integrated packed-bed rock TES system. Previous studies [2,10,11] considered foil-based CSP plants with only SCORC systems. No previous works addressed the selection of these ORC architectures for such plant.
- An evaluation of the techno-economic feasibility of different ORC configurations, including the TLORC and PEORC systems, for a CSP plant considering the effects of the solar field's efficiency and cost, and parameters of the power system. No previous works evaluated the techno-economic feasibility of the TLORC and PEORC systems for CSP applications.
- An evaluation of the techno-economic feasibility of different ORC configurations for geothermal applications by determining their feasible regions considering the effects of the cost of geothermal energy and power system parameters. A previous study [4] evaluated the techno-economic feasibility of using PEORC systems for geothermal applications by optimizing the thermodynamic cycle and by estimating relevant economic parameters, such as the specific investment cost of the system and the levelized cost of electricity. The proposed approach presented in this paper based on the development of a selection diagram is novel.

Section 2 explains the different models and methods. Section 3 describes the different results achieved by the techno-economic analyses and Section 4 discusses the conclusions of the work.

2. Methods

2.1 System description

A techno-economic comparison among trilateral, partial evaporation and conventional sub-critical ORC systems powered by foil-based CSP and geothermal heat, respectively, was carried out. All the numerical analyses were conducted using the software Engineering Equation Solver (EES) [12]. For the CSP plant, a foil-based concentrating solar collector powered ORC unit was investigated in the present work for electricity production. Fig. 1 shows a schematic *T*-s diagram of a regenerative organic Rankine cycle, a trilateral organic Rankine cycle and a partial evaporation organic Rankine cycle. Based on techno-economic optimisation results by Desai et al. [10], the packed-bed rock thermocline storage was used as thermal energy storage for the foil-based solar field technology. Different modes of plant operation, the calculation procedure at each time step and parameters for the annual simulations of the CSP plant with packed-bed rock thermocline TES were based on our previous work [10]. The calculation of the optimum solar multiple and optimum LCOE was based on our previous work [10], and the annual energy production for the TLORC and PEORC cases were calculated based on the optimum value of solar multiple and the corresponding capacity factor obtained for the SCORC case. For CSP plants with SCORC, cyclopentane was used as a working fluid for the ORC power system based on the techno-economic optimisation results by Desai et al. [11] for the foil-based solar field technology. For CSP powered TLORC and PEORC plants with design condition solar field outlet temperature of 278 °C and 208 °C, toluene and cyclopentane, respectively, were used as working fluid for the ORC power system. This is because toluene has higher critical temperature (318.6 °C) than cyclopentane (238.57 °C), allowing high temperature operation of TLORC and PEORC for the 278 °C solar field outlet temperature case. Furthermore, the current foil-based CSP field and the receiver is designed for district heating applications. Therefore, there is an enhancement potential for their thermal performances. In addition, foil-based CSP systems are very easy to manufacture compared to the traditional mirror based CSP systems. As a result, in future, based on the mass production, a significant cost reduction is expected. In this work, a foil-based solar collector system with a medium-scale manufacturing cost of 150 €/m2 and with an enhancement of the heat loss coefficient of 20 % was considered.

A geothermal energy powered ORC unit for electricity production was also analysed. For low to medium temperature geothermal energy based SCORC, TLORC and PEORC systems, two promising working fluids, R245fa and cyclopentane, were used as a working fluid for the ORC power system based on the techno-economic optimisation results by Tammone et al. [4]. While the same overall approach to evaluate the thermodynamic and economic performance of the systems was adopted, the sizing of the systems was done differently for the two energy sources. For the CSP plant, the gross power output of the system was assigned and the solar field area was obtained as a result, while the heat source mass flow rate and temperature, and consequently the available heat input, were fixed for the geothermal plant.

2.2 Thermodynamic analysis

The design condition ORC expander shaft power output ($\dot{P}_D$) was determined as follows:

$$\dot{P}_D = \dot{m}_D \cdot \Delta h_{is,D} \cdot \eta_{is,D} \quad (1)$$

where $\dot{m}_D$ is the ORC working fluid mass flow rate at design condition, $\eta_{is,D}$ is the ORC expander isentropic efficiency at design condition, and $\Delta h_{is,D}$ is the ORC expander isentropic specific enthalpy drop at design condition.

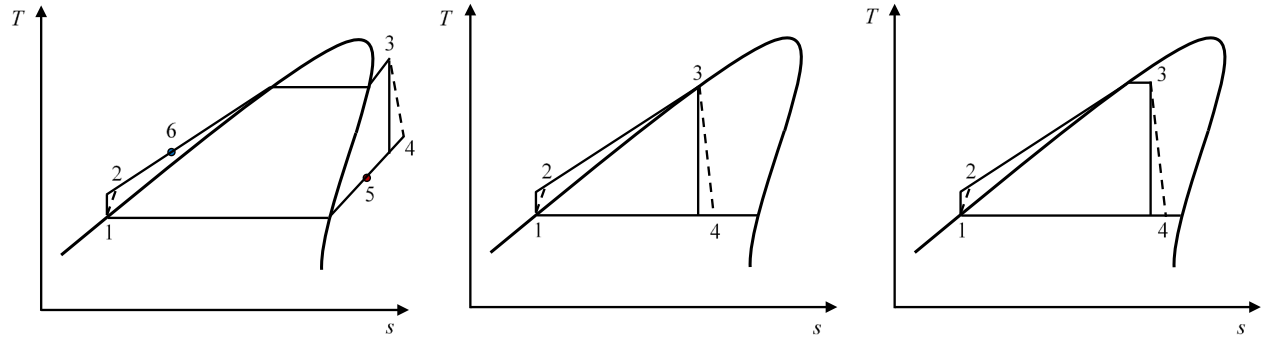

Fig. 1. T-s diagram of (a) regenerative organic Rankine cycle, (b) trilateral organic Rankine cycle and (c) partial evaporation organic Rankine cycle.

The design gross electric power output of the ORC power system ($\dot{P}_{gross,D}$) was calculated as follows:

$$\dot{P}_{gross,D} = \dot{P}_D \cdot \eta_{mech} \cdot \eta_{gen,D} \quad (2)$$

where $\eta_{gen,D}$ and η_{mech} are the design generator and mechanical efficiencies, respectively.

The design net power output of the ORC power system ($\dot{P}_{net,D,PS}$) was determined as follows:

$$\dot{P}_{net,D,PS} = \dot{P}_{gross,D} - \dot{P}_{ORC,FeedPump,D} \quad (3)$$

where $\dot{P}_{ORC,FeedPump,D}$ is the ORC power system feed pump power consumption at design condition.

The net power output of the complete plant ($\dot{P}_{net,D,plant}$) was determined as follows:

$$\dot{P}_{net,D,plant} = \dot{P}_{net,D,PS} - \dot{P}_{other,D,Aux} \quad (4)$$

where $\dot{P}_{other,D,Aux}$ is the power requirement of other auxiliaries, which are parasitic electricity use for the solar field, TES pump and antifreeze system pumping for CSP plants, and heat source pump and cooling water pump consumption for geothermal plants.

For the CSP plant, the methods and models used to calculate the part-load performance of the different components of the plant, in order to calculate annual output, were the same as those presented in Desai et al. [10]. The code of the ORC power system was validated in our previous work [2] using the data of the n-pentane based Arizona Public Service Saguaro plant in the USA [13] and the Turboden [14] manufacturer catalogue. The results indicate that for the power system loads down to 40%, the maximum absolute deviation in the gross thermal efficiency of the SCORC system is about 0.5 %-points and 0.28 %-points for n-pentane and hexamethyldisiloxane, respectively. For loads below 40 %, the maximum absolute deviation in the gross thermal efficiency is 2.2% and 1% for n-pentane and hexamethyldisiloxane, respectively. For the geothermal plant, a number of equivalent full load operating hours per year were considered to calculate the annual energy production of the plant. The input data required for the thermodynamic analysis of the CSP and geothermal energy powered plants are given in Table 1.

2.3. Economic analysis

The capital investment costs of the ORC feed pump, condenser, electrical generator and TES tanks (for CSP plants) were calculated as follows:

$$C = C_0 \cdot \left(\frac{Capacity}{Capacity_0}\right)^e \quad (5)$$

Table 1. Data required for thermodynamic analysis of the system.

Input parameters for the CSP system	*Value*
Solar field's efficiency parameters	Optical efficiency of solar field ($\eta_{o,SF}$) = 0.833; Solar field heat-loss coefficient based on the aperture area ($U_{l,SF}$) = 0.85 W/(m^2·K) and 0.68 W/(m^2·K) (by improvements)
Solar field heat transfer fluid	Therminol 55
Solid filler for packed-bed rock thermal energy storage	Quartzite rock
Packed-bed porosity	22 % [15]
Solid filler particle diameter	0.015 m [15]
Ambient temperature at design condition	30 °C
Gross electrical power output of the CSP plant	1 MW$_e$
Electricity production penalty due to start-up and shut-down procedures, and heat-losses through piping and pressure losses	10 % of net power output [16]
Parasitic electricity use for CSP field, TES pump and antifreeze system pumping	7 % of net power output [13]
Efficiency of TES electric heating unit	0.9
Input parameters for the geothermal energy powered system	*Value*
Mass flow rate of geothermal brine	100 kg/s
Pressure drop in geothermal brine	300 kPa
Isentropic efficiency of geothermal brine circulation pump and cooling water pump	0.75
General input parameters	*Value*
Design efficiency of generator and copper loss-fraction	0.93 and 0.43 [17]
Design efficiency of turbine (for SCORC)	Based on Astolfi and Macchi [18]
Design isentropic efficiency of ORC feed pump	0.7 [19]

where C_0 and $Capacity_0$ are the capital investment cost and the capacity for the reference system, respectively, and e is a scaling factor.

The SCORC axial turbine cost (C_T) was evaluated as follows [19]:

$$C_T = C_0 \cdot \left(\frac{n}{n_0}\right)^{e_1} \cdot \left(\frac{SP}{SP_0}\right)^{e_2} \quad (6)$$

where C_0, SP_0, and n_0 are the capital investment cost, the size parameter and the number of turbine stages for the reference turbine, respectively, and e_1 and e_2 are the scaling factors. In the present work, for each turbine stage, the maximum value of the specific isentropic enthalpy change was taken as 65 kJ/kg [19].

The capital investment costs of the primary heat exchanger and regenerator were calculated as follows [19]:

$$C_{eva/reg} = C_0 \cdot \left(\frac{UA}{UA_0}\right)^{e} \cdot z \quad (7)$$

$$z = (10)^{(z_1 + z_2 \cdot log\, p + z_3 \cdot log^2 p)} \quad (8)$$

where C_0 and UA_0 are the capital investment cost and the UA value (product of overall heat transfer coefficient and heat transfer area) of the reference system, respectively, p is pressure, and e is a scaling factor.

The annualised value for the capital investment cost of the complete plant (AC_{system}) was calculated as follows:

$$AC_{system} = \left(C_{system} \cdot CRF + C_{O\&M}\right) \quad (9)$$

$$CRF = d \cdot \frac{(1+d)^k}{((1+d)^k)-1} \quad (10)$$

where C_{system} is the capital investment cost of the complete plant, $C_{O\&M}$ is the annual operation and maintenance cost of the plant, k is the lifetime of the plant, d is the discount rate, and CRF is the capital recovery factor. The input data required for the economic analysis of the CSP and geothermal energy powered plants are given in Table 2.

The LCOE was determined as given below:

$$LCOE = \frac{AC_{system}}{E_{power}} \quad (11)$$

where E_{power} and AC_{system} are the net annual electricity generation and the annualised capital investment cost for the plant, respectively.

3. Results and discussion

The selection among the SCORC, TLORC and PEORC is significantly affected by the expander efficiency and the cost of the power system. The variations of relative power system costs per unit of design net power output $((C_{PS,total}/\dot{P}_{net,D,PS})_{TLORC}/(C_{PS,total}/\dot{P}_{net,D,PS})_{SCORC})$ as a function of relative isentropic efficiency of expanders $(\eta_{is,D,TLORC}/\eta_{is,D,SCORC})$ are presented in Fig. 2 representing a selections diagram that helps to identify the optimal configuration of an ORC power system, in this case for current and future foil-based CSP plants. The selection diagram consists of two zones divided by a solid black line for the current plants and a solid blue line for the future plants representing the condition of equal LCOE for the SCORC and TLORC plants. In order to obtain this condition, the isentropic efficiency of the expander for the TLORC was varied and the corresponding specific cost of the power system $(C_{PS,TLORC} = (C_{PS,total}/\dot{P}_{net,D,PS})_{TLORC})$ was determined, in order to get the same value of LCOE as for the SCORC system. The vertical dotted black line represents the condition of equal specific power system cost per unit of design net power output for the TLORC and SCORC systems. The region on the left hand side of the solid line of the selection diagram indicates the conditions resulting in the TLORC system being the optimal plant, whereas the region on the right hand side of the solid line represents the conditions resulting in the SCORC system being the optimal plant. As the TLORC architecture is expected to result in a more costly ORC power system, a possible techno-economically feasible region for the TLORC system is located to the right of the dotted line and to the left of the solid line. If such region does not exist, there is no economic benefit in selecting the TLORC power system over the SCORC power system.

Fig. 2 indicates that the prospects for the TLORC system improves for the future solar field scenario, which is reflected by a movement of the LCOE equal line to the right for the future solar field scenario. This is because for medium to high temperature CSP applications (unlike low temperature geothermal applications), the thermal efficiency of the TLORC system ($\dot{P}_{net,D,PS}/\dot{Q}_{in}$) is lower than that of the SCORC system, and therefore the reduction in the specific cost of the solar field (€/kW$_{th}$) leads to positive impact in terms of LCOE for the CSP powered TLORC system. The results also suggest that for a solar field outlet temperature

Table 2. Data required for economic analysis of the system.

Input parameters for the concentrated solar energy powered system	*Value*
Foil-based solar field and HTF system cost	For current plants: 250 €/m^2; For future plants: 150 €/m^2
Site development and land cost	4.7 €/m^2 of land [20]
Place	Antofagasta, Chile
Thermal energy storage HTF and rock cost	Therminol 55: 2.7 €/kg [21]; Quartzite rock : 0.556 €/kg [15]
Cost parameters of thermal storage tank, including insulation and foundation	C_0 = 7,932,160 € [22], $Capacity_0$ = 30,844 m^3 [22] and e = 0.85
Thermal oil to molten salt (Hitec XL) heat exchanger cost parameters	C_0 = 4,580,235 € [22], $Capacity_0$ = 133 MW$_{th}$ [22] and e = 0.85
Balance of TES system cost, including TES system pump	14 % of the TES system cost [22]
Miscellaneous cost for the plant	144 €/kW$_e$ [20]
Cost of annual O&M	Fixed cost – 1.4 % of the total investment cost; Variable cost – 2.8 €/MWh$_e$
Input parameters for geothermal energy powered system	*Value*
Cost of the geothermal energy resource	6,000,000 € (for the base case)
Cost of annual O&M	2 % of the total investment cost
Number of equivalent full load operation hours per year	8000 h
General input parameters	*Value*
Regenerator and evaporator cost parameters	Evaporator: C_0 = 1570 k€, UA_0 = 4,000 kW/K, z_1 = 0.03881, z_2 = – 0.11272, z_3 = 0.08183, and e = 0.9 [19] Regenerator: C_0 = 272 k€, UA_0 = 650 kW/K, z_1 = – 0.00164, z_2 = – 0.00627, z_3 = 0.0123, and e = 0.9 [19]
SCORC turbine cost parameters	C_0 = 1,287,810 €, n_0 = 2, SP_0 = 0.18 m, e_1 = 0.85 and e_2 = 1.1 [19]
Electrical generator cost parameters	C_0 = 209,400 €, $Capacity_0$ = 5,000 kW$_e$ and e = 0.67 [19]
Gear box cost	40 % of the generator cost [19]
Condenser cost parameters	C_0 = 13,075 €, $Capacity_0$ = 50 kW$_{th}$ and e = 0.76 [23]
Boiler feed pump cost parameters	C_0 = 14,658 €, $Capacity_0$ = 200 kW and e = 0.67 [19]
Balance of ORC unit cost	40 % of the ORC unit's component costs [19]
Discount rate	3 %
Lifetime	25 y

Note: All the parameters for the cost correlations have been converted using the CEPCI to the value of year 2018.

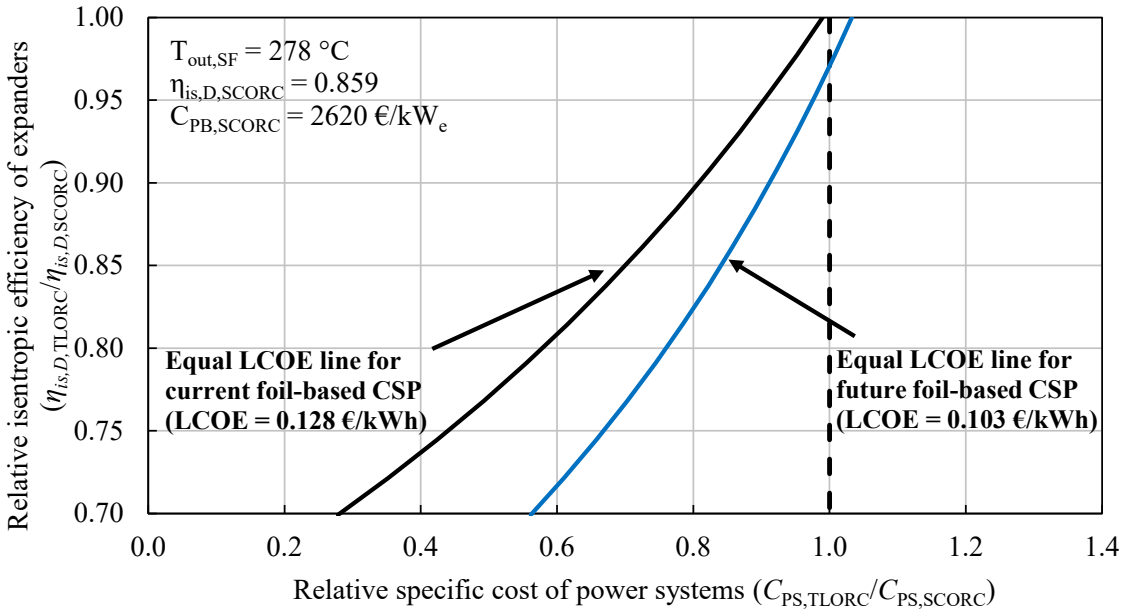

Fig. 2. Selection diagram for current and future foil-based concentrating solar collector powered subcritical organic Rankine cycle and trilateral organic Rankine cycle systems.

of 278 °C, the TLORC cannot compete with the SCORC (see Fig. 2), while for a solar field outlet temperature of 208 °C, a practically feasible region exists for the TLORC (see Fig. 3). However, the LCOE is about 22 % higher for this case compared to the solar field outlet temperature of 278 °C, making it a less competitive technology. Moreover, for a solar field outlet temperature of 208 °C, in order to be techno-economically attractive, the TLORC can only have a 10 % increase in the relative cost of the power system and a reduction in the expander isentropic efficiency up to 7 % compared with the SCORC. Overall, the results indicate that it is questionable if the TLORC system would bring any economic advantages for medium to high temperature CSP applications.

As previously mentioned, the use of the PEORC instead of the TLORC can reduce the cost of the power system and increase the expander efficiency. Fig. 4 depicts a selection diagram for foil-based CSP powered SCORC and PEORC systems. For comparison, the lines of equal LCOE both for the TLORC and the PEORC are included. Despite of having lower values of the relative specific cost of power systems and

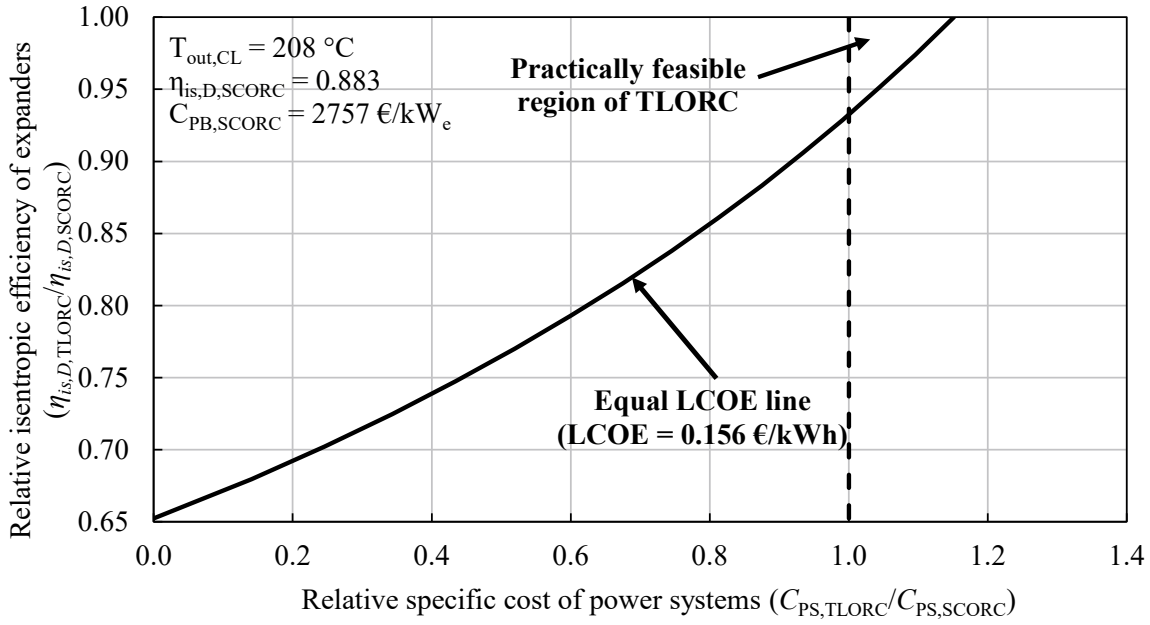

Fig. 3. Selection diagram for current foil-based concentrating solar collector powered subcritical organic Rankine cycle and trilateral organic Rankine cycle systems.

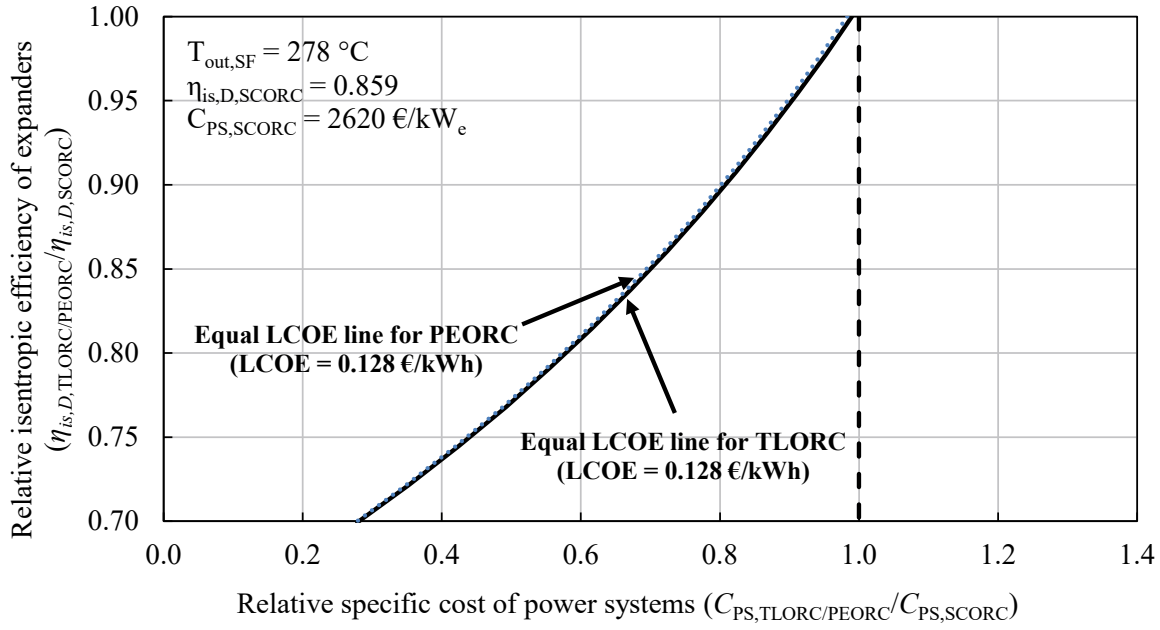

Fig. 4. Selection diagram for foil-based concentrating solar collector powered subcritical organic Rankine cycle and trilateral/partial evaporation organic Rankine cycle systems.

higher values of the relative isentropic efficiency of the expanders than those of the TLORC system, the results suggest that the PEORC does not offer any economic advantages over the SCORC, as the practically feasible region does not exist.

A corresponding selection diagram for the TLORC using two different working fluids for the geothermal case is presented in Fig. 5. In this case, R245fa is used as a working fluid for the SCORC system. The results indicate that the TLORC would be the preferably system from a techno-economically perspective only if the specific cost for the TLORC is lower or equal to that of the SCORC and the penalty in the isentropic efficiency of TLORC is lower than 10 %.

The effects of the cost of the geothermal energy resource on the selection diagram is shown in Fig. 6. As expected, a high cost of the geothermal heat source is favourable for the TLORC system, as the higher investment cost to a larger degree is balanced by the increased annual energy production for the TLORC than the SCORC when evaluating the LCOE.

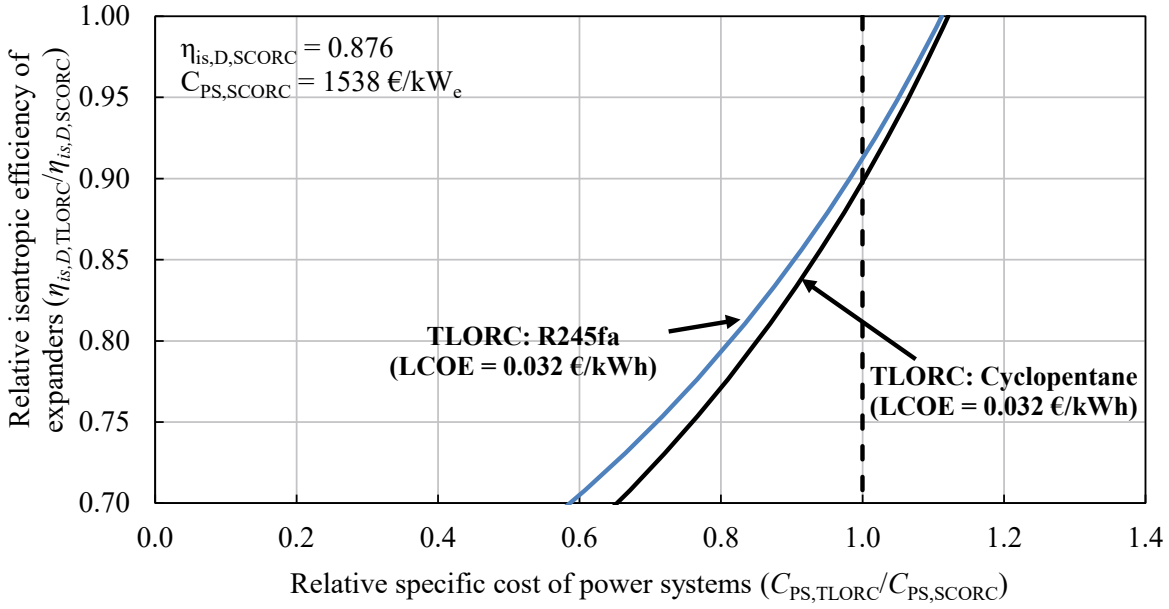

Fig. 5. Selection diagram for geothermal energy powered subcritical organic Rankine cycle and trilateral organic Rankine cycle systems.

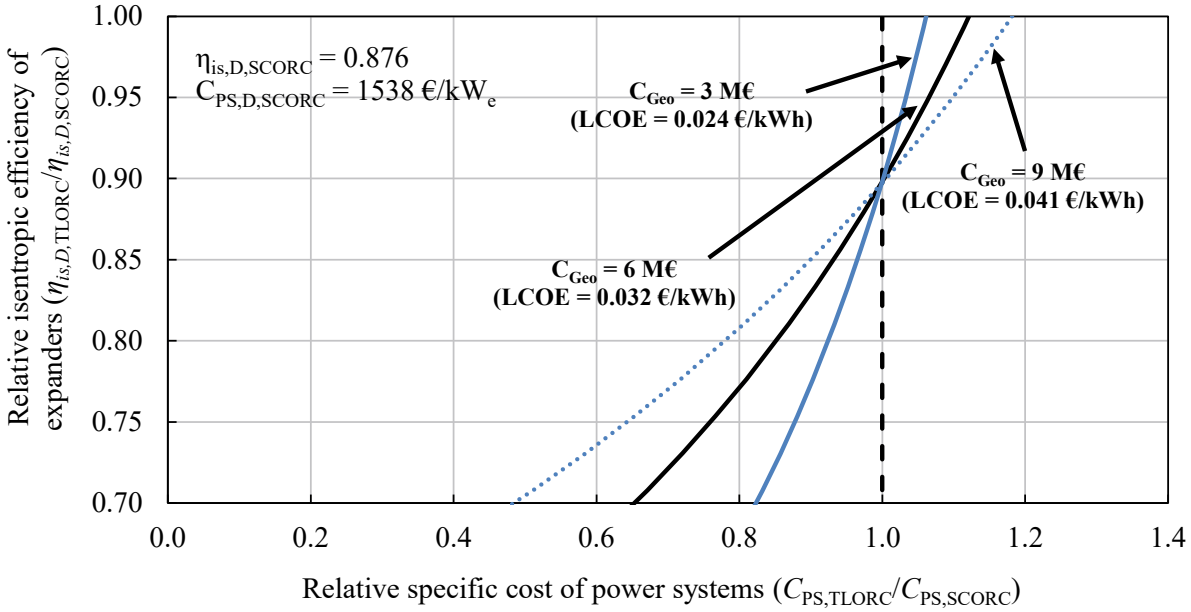

Fig. 6. Effects of cost of geothermal energy resource on the selection diagram for geothermal energy powered subcritical organic Rankine cycle (with R245fa as working fluid) and trilateral organic Rankine cycle systems (with cyclopentane as working fluid).

Fig. 7 presents the effects of condensation temperature on the selection diagram for geothermal energy powered SCORC and TLORC systems. As expected, a high value of condensation temperature is favourable for TLORC system because it will lead to a better matching between the heat source and TLORC working fluid profiles for a geothermal heat source with a fixed brine temperature of 150 °C and a fixed brine re-injection temperature of 70 °C.

Fig. 8 shows a selection diagram for geothermal energy powered SCORC and PEORC systems. Lines of equal LCOE are included both for the TLORC and PEORC systems. As mentioned earlier, PEORC systems are more likely to get a lower relative specific cost of the power system and a higher value of the relative isentropic efficiency of the expander compared to the TLORC system, hence being more promising.

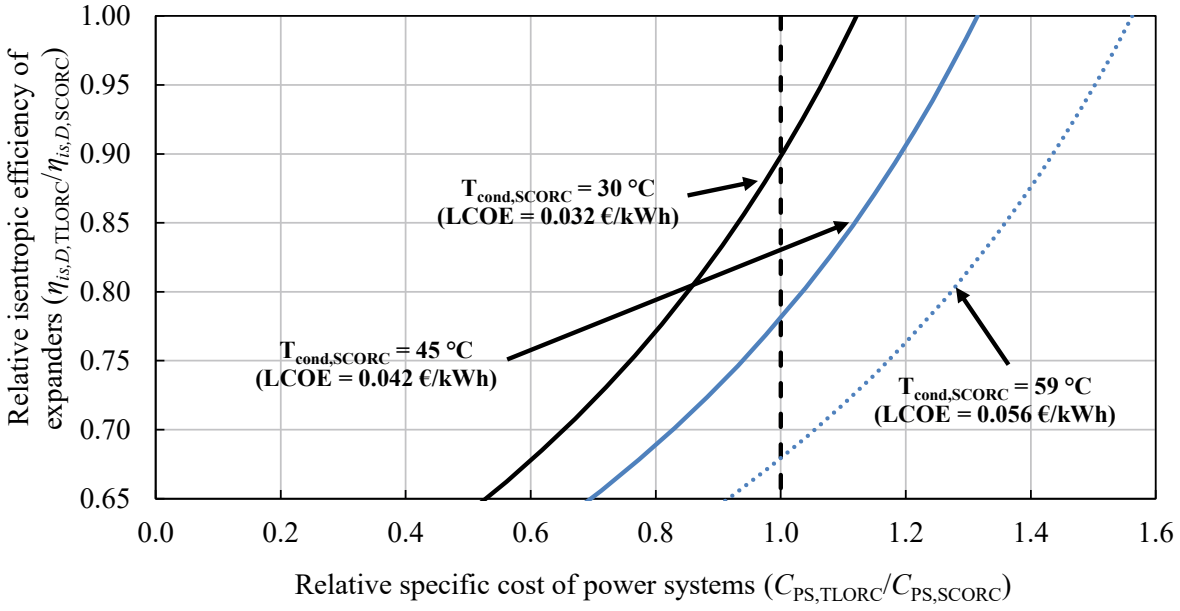

Fig. 7. Effects of condensation temperature on selection diagram for geothermal energy powered subcritical organic Rankine cycle (with R245fa as working fluid) and trilateral organic Rankine cycle systems (with cyclopentane as working fluid).

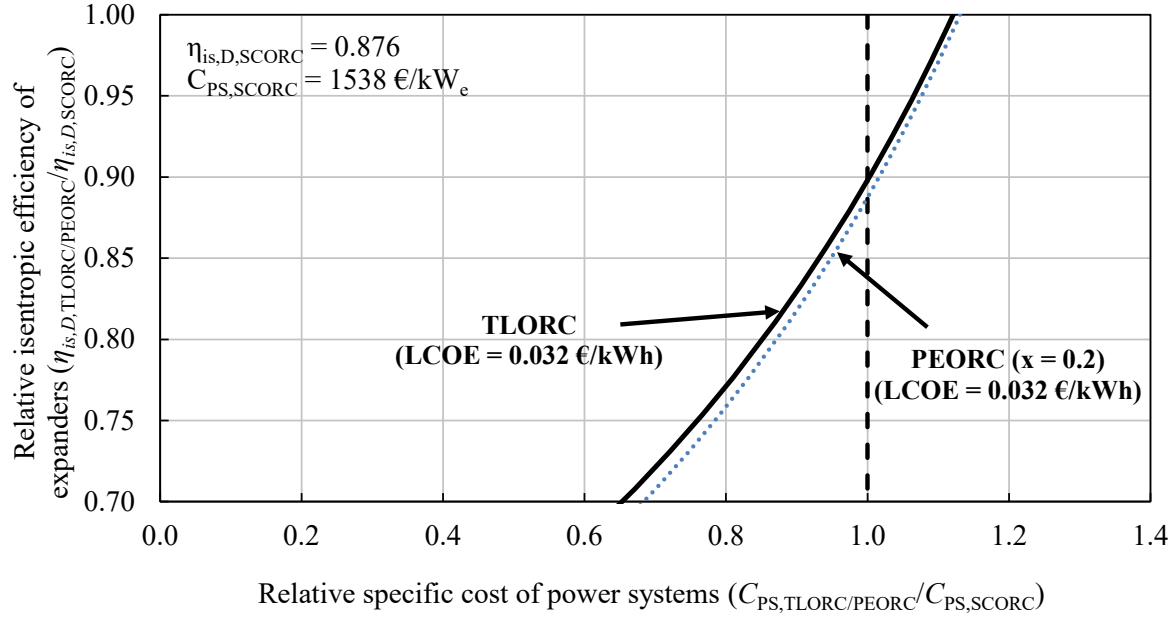

Fig. 8. Selection diagram for geothermal energy powered subcritical organic Rankine cycle (with R245fa as working fluid) and trilateral/partial evaporation organic Rankine cycle systems (with cyclopentane as working fluid).

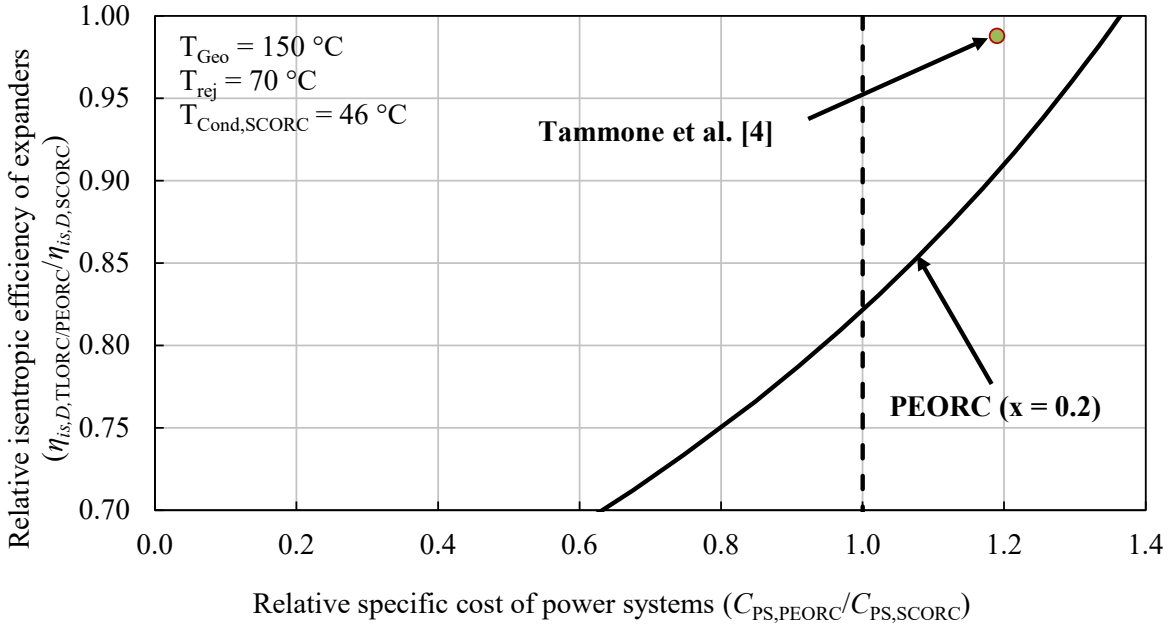

Fig. 9. Comparison with literature result [4] for geothermal energy powered subcritical organic Rankine cycle (with R245fa as working fluid) and partial evaporation organic Rankine cycle system (with cyclopentane as working fluid).

In order to show the application of the proposed selection diagrams, the relative isentropic efficiency of expanders and relative specific cost of power systems based on the work of Tammone et al. [9] were applied. Fig. 9 depicts the case with a geothermal brine temperature (T_{geo}) of 150 °C, a brine re-injection temperature (T_{rej}) of 70 °C, a cost of the geothermal energy resource of 6 M€ and estimations of the expander isentropic efficiency for both the SCORC and PEORC system following Astolfi et al. [16] (without considering any penalty for the PEORC expander). It can be observed that the design point falls in the practically feasible region of the PEORC system, and therefore, for the considered case, the PEORC system is preferred over the SCORC system, which was also concluded by Tammone et al. [4].

4. Conclusions

In this paper, a comparative analysis among the subcritical, trilateral and partial evaporation organic Rankine cycle based systems powered by concentrated solar power integrated packed-bed rock thermal energy storage and geothermal energy, respectively, was presented. A novel approach based on the development of a selection diagram, which captures the variations of relative specific power system cost as a function of relative isentropic efficiency of the expander, was proposed. The selection diagram represents the condition of equal levelized cost of electricity for trilateral and partial evaporation organic Rankine cycle based power systems and the subcritical organic Rankine cycle based power system, respectively, allowing to identify the optimal cycle architecture of the plant once the system cost and the expander isentropic efficiency are known. The results suggest that for concentrated solar power plants, from a techno-economic perspective, the subcritical organic Rankine cycle system is the preferred choice over the trilateral and partial evaporation organic Rankine cycles. As for the geothermal energy powered plants, the results indicate that the trilateral organic Rankine cycle system can be the preferable option over the subcritical organic Rankine cycle system, provided its increase in the specific cost does not exceed 10 % and its penalty in expander isentropic efficiency does not exceed 10 %. Finally, it needs to be stressed that high condensation temperatures, which for example would be the case for plants with air-cooled condensers and co-generation plants using a back-pressure turbine, are favourable for the trilateral and partial evaporation organic Rankine cycles for geothermal applications.

Acknowledgments

The research presented in this paper was developed as part of the project “Widespread use of geothermal energy in East Africa” (File No. 20-06-DTU), funded by the Ministry of Foreign Affairs of Denmark and administrated by Danida Fellowship Centre. The financial support is gratefully acknowledged.

Nomenclature

C Cost (€)

C_{SCORC} Specific cost of the subcritical organic Rankine cycle based power system (€/kW$_e$)

C_{TLORC} Specific cost of the trilateral organic Rankine cycle based power system (€/kW$_e$)

CRF capital recovery factor (y^{-1})

d discount rate (%)

k lifetime of the plant (y)

$LCOE$ levelized cost of electricity

$\dot{P}$ power (kW$_e$)

x dryness fraction (-)

$U_{l,SF}$ solar collector field heat-loss coefficient (W/(m^2·K))

Greek symbols

η efficiency

Subscripts and superscripts

D design

gen generator

is isentropic

o optical

out outlet

PS power system

rej re-injection

SF solar field

Abbreviations

CSP	concentrated solar power
ORC	organic Rankine cycle
PEORC	partial evaporation organic Rankine cycle
SCORC	subcritical organic Rankine cycle
TES	thermal energy storage
TLORC	trilateral organic Rankine cycle

References

[1] Pranov H., Matschuk M., Laminate solar concentrator, U.S. Patent Appl. 16/081, 532, Heliac Aps, 2019.

[2] Desai N.B., Pranov H., Haglind F., Techno-economic analysis of a power generation system consisting of a foil-based concentrating solar collector and an organic Rankine cycle unit. In Proceedings of the 32nd International conference on efficiency, cost, optimization, simulation and environmental impact of energy systems (ECOS 2019), Wroclaw, Poland: 2019.

[3] Smith, I. K., Development of the trilateral flash cycle system Part 1 : fundamental considerations, Proceedings of the Institution of Mechanical Engineers, Part A: Journal of Power and Energy 1993;207(3):179–194.

[4] Tammone, C., Pili, R., Indrehus, S., Haglind, F., Techno-economic analysis of the partial evaporation organic Rankine cycle systems for geothermal applications. In Proceedings of the 6th International Seminar on ORC Power Systems, Munich, Germany:2021.

[5] Fischer, J., Comparison of trilateral cycles and organic Rankine cycles, Energy 2011;36(10): 6208–6219.

[6] Lai, N. A., Fischer, J., Efficiencies of power flash cycles, Energy 2012;44(1):1017–1027.

[7] Lecompte, S., Lemmens, S., Verbruggen, A., Van Den Broek, M., De Paepe, M., Thermo-economic comparison of advanced organic Rankine cycles, Energy Procedia 2014;61:71–74.

[8] Lecompte, S., Huissene, H., Van Den Broek, M., De Paepe, M., Methodical thermodynamic analysis and regression models of organic Rankine cycle architectures for waste heat recovery, Energy 2015;87:60–76.

[9] Yari, M., Mehr, A. S., Zare, V., Mahmoudi, S. M. S., Rosen, M. A., Exergoeconomic comparison of TLC (trilateral Rankine cycle), ORC (organic Rankine cycle) and Kalina cycle using a low grade heat source. Energy 2015;83:712–722.

[10] Desai, N. B., Mondejar, M. E., Haglind, F., Techno-economic analysis of two-tank and packed-bed rock thermal energy storages for foil-based concentrating solar collector driven cogeneration plants, Renew. Energy 2022;186:814–830.

[11] Desai N. B., Pranov H., Haglind F., Techno-economic analysis of a foil-based concentrating solar collector driven electricity and fresh water generation system, Renew. Energy 2021;165:642–656.

[12] Klein S., Software F-Chart, EES-Engineering Equation Solver V10.478, 2018.

[13] National Renewable Energy Laboratory (NREL). System Advisor Model – Available at: <www.sam.nrel.gov/> [accessed 15.12.2018].

[14] Turboden. Available at: <www.turboden.com> [accessed 22.11.2018].

[15] Niedermeier K., Marocco L., Flesch J., Mohan G., Coventry J., Wetzel T., Performance of molten sodium vs. molten salts in a packed bed thermal energy storage, Appl. Therm. Eng. 2018;141:368–377.

[16] Manzolini G., Bellarmino M., Macchi E., Silva P., Solar thermodynamic plants for cogenerative industrial applications in southern Europe, Renew. Energy 2011;36(1):235–243.

[17] Haglind F., Elmegaard B., Methodologies for predicting the part-load performance of aero-derivative gas turbines, Energy 2009;34(10):1484–1492.

[18] Astolfi M., Macchi E., Efficiency correlations for axial flow turbines working with non-conventional fluids. In Proceedings of the 3rd International Seminar on ORC Power Systems, Brussels, Belgium: 2015;12–14.

[19] Astolfi M., Romano M.C., Bombarda P., Macchi E., Binary ORC (Organic Rankine Cycles) power plants for the exploitation of medium–low temperature geothermal sources–Part B: Techno-economic optimization, Energy 2014;66:435–446.

[20] IIT Bombay, Solar Thermal Simulator Version 2.0, 2014.

[21] Cocco D., Serra F., Performance comparison of two-tank direct and thermocline thermal energy storage systems for 1 MWe class concentrating solar power plants, Energy 2015;81:526–536.

[22] Herrmann U., Kelly B., Price H., Two-tank molten salt storage for parabolic trough solar power plants, Energy 2004;29(5–6):883–893.

[23] Lemmens S., Cost engineering techniques and their applicability for cost estimation of organic Rankine cycle systems, Energies 2016;9(7):485.